A fluorescence based method for the quantification of surface functional groups in closed micro- and nanofluidic channels

Yu Wang,[1] Rachel D. Lowe,[1] Yara X. Mejia,[1] Holger Feindt,[2] Siegfried Steltenkamp,[2] and Thomas P. Burg[1,a)]
[1]*Max Planck Institute for Biophysical Chemistry, Am Fassberg 11, 37077 Göttingen, Germany*
[2]*Micro Systems Technology (MST), Center of Advanced European Studies and Research (caesar), Ludwig-Erhard-Allee 2, 53175 Bonn, Germany*

(Received 14 December 2012; accepted 4 April 2013; published online 22 April 2013)

Surface analysis is critical for the validation of microfluidic surface modifications for biology, chemistry, and physics applications. However, until now quantitative analytical methods have mostly been focused on open surfaces. Here, we present a new fluorescence imaging method to directly measure the surface coverage of functional groups inside assembled microchannels over a wide dynamic range. A key advance of our work is the elimination of self-quenching to obtain a linear signal even with a high density of functional groups. This method is applied to image the density and monitor the stability of vapor deposited silane layers in bonded silicon/glass micro- and nanochannels. © *2013 AIP Publishing LLC* [http://dx.doi.org/10.1063/1.4802270]

I. INTRODUCTION

Microfluidic devices are continually being developed as platforms for diagnostics and biochemical analysis as they provide many advantages in terms of sample consumption, liquid handling precision and throughput.[1,2] Surface functionalization is often critical to the functionality of microfluidic devices in these applications. For example, surface immobilization of DNA[3] or proteins[4] recognizing specific ligands is required in label-free biosensors and microfluidic immunoassays.[5,6] Conversely, surface attachment of molecules which reduce non-specific binding is often crucial in biomolecular separation and pre-concentration.[7] As such, surface functionalization plays a key role in preserving the activity of complex molecules and needs to be well characterized and reproducible. In this paper, we describe a new fluorescence imaging method for the characterization of surface modifications inside assembled micro- and nanofluidic channels.

Common non-covalent surface modification strategies which have been employed in the context of microfluidic devices include physisorption of polyelectrolytes[8] or natural adhesive groups, such as 3,4-dihydroxy-L-phenylalanine (DOPA),[9] and the self-assembly of lipid bilayers and thiols.[10–12] These non-covalent linkers are attractive due to their ease of use in microfluidic systems by one-step flow-through delivery. Nevertheless, covalent coupling is often preferred when high stability of the surface or a high density of functional groups is required. Silane coupling agents have gained widespread popularity as covalent linkers that can be used for the functionalization of silicon, glass, and polymers commonly used in microfluidics.[13–17] However, the reproducible deposition of high-quality silane layers inside microfluidic channels is often difficult, especially to researchers new to the field.[13] This is predominantly due to the combination of experimental challenges associated with flow-through systems and a simultaneous shortage of surface analysis methods able to provide validation and feedback in closed microfluidic

a)Author to whom correspondence should be addressed. Electronic mail: tburg@mpibpc.mpg.de. Tel.: +49-551-201-1187. Fax: +49-551-201-1577.

systems. First among the experimental challenges is the requirement for clean surfaces and high purity reagents. Both are not always trivial to ensure in microfluidics, as assembled channel surfaces cannot be as easily rinsed, dried, and plasma-cleaned as open samples. Flow-through systems are also more susceptible to cross-contamination of reagents by dispersion in external tubing and connections, and they are highly susceptible to clogging by particulates that would not be of concern in open systems.

Many of these challenges associated with the silane modification of microfluidic systems can be overcome by systematic optimization of protocols and the chemistry involved. Yet, such systematic optimization requires accurate means of characterization, and current surface analysis methods are not able to provide this feedback due to the inaccessible nature of assembled microfluidic channels. Routine methods used for the characterization of open surfaces include atomic force microscopy (AFM),[18] X-ray photoelectron spectroscopy (XPS),[19] contact angle measurement and ellipsometry,[20] which cannot be readily implemented in the microfluidic system. Previous studies have demonstrated silane layer characterization for microfluidic applications after silanization but before bonding/closing of the channels.[21,22] However, this method alters the bonding chemistry and potentially compromises the strength or uniformity of the bond. In addition, pre-bonding characterization methods do not allow for the monitoring of regenerated microchannel surfaces.

Surface characterization may also be performed using surface plasmon resonance (SPR),[23] wavelength interrogated optical sensors (OWS),[24] and quartz crystal microbalance (QCM).[25] However, these methods cannot provide measurements inside already assembled micro- and nanofluidic channels, unless the fluidic device has been engineered specifically for that purpose. Alternatively, methods based on cleavable labels that are quantified using spectroscopy are also limited due to the small number of molecules in the microfluidic eluent.[26,27] Furthermore, such methods provide no information about spatial homogeneity and the presence of aggregates. In contrast, fluorescence microscopy is a widely applicable detection method with high sensitivity and ease of use.[3,6,27] The binding of fluorescent ligands has been commonly used for verifying surface functionalization.[14,28] However, these studies have only qualitatively compared silanized and non-silanized surfaces, but have not quantified the fluorescent intensity of the resulting layers.[20,29–31] Fluorescence Recovery after Photobleaching (FRAP) has been used previously to characterize lipid coatings on solid surfaces with only a subset of the lipids fluorescently labeled.[12] Nonetheless, this method cannot be applied to non-lipid coatings, such as organosilanes, as the functional groups are not mobile. In addition, an important problem in quantitative fluorescence-based measurements in non-lipid systems is the non-linearity of fluorescence intensity introduced by self-quenching at high dye concentration.[32,33]

Here, we demonstrate a new method, which enables quantitative measurements of surface functional group density in micro- and nanofluidic channels by fluorescence microscopy. The new method overcomes self-quenching limitations using a mixture of fluorescent and non-fluorescent molecules, which compete for the available functional groups on the surface. We first demonstrate the importance of limiting dye-to-dye distance at high area density of functional groups and subsequently establish a set of conditions that ensures a linear correlation between fluorescent intensity and surface coverage. The potential for absolute measurements is confirmed by comparison to conventional surface labeling cleavage techniques on centimeter-scale samples.

The ability to quantitate *in situ* is a significant advance over the mere detection of the presence or absence of the desired functional groups. Quantitation allows for the optimization of the binding capacity of the surface in order to maximize the capture of targets. Additionally, this method helps to standardize assays that rely on the measurement of fluorescent intensities (like immunoassays) by eliminating errors due to chip-to-chip surface variability. Finally, this technique can aid in the assessment of the success and efficiency of surface regeneration strategies for sequential experiments on the same microfluidic chip.

As an application of the optimized fluorescent labeling method, we present a detailed characterization of mono- and trialkoxyaminosilane layers deposited by a simple vapor-based batch process inside assembled microfluidic devices. Although in this study we have used vapor

deposition of aminosilanes, the described principles can also be amended for flow through liquid silanization procedures and for other coupling agents and a wide range of other functional groups.

II. MATERIALS AND METHODS

A. Chemicals

3-aminopropyl trimethoxysilane (APTMS) and 3-aminopropyl dimethylmethoxysilane (APDMMS) were purchased from Sigma-Aldrich, Steinheim, Germany. Alexa Fluor® 555 carboxylic acid, succinimidyl ester (AF555-NHS-ester) was obtained from Invitrogen GmbH, Darmstadt, Germany. EZ-Link® sulfosuccinimidyl 6-(biotinamido) hexanoate (sulfo-NHS-biotin) was purchased from Pierce Biotechnology, Rockford, USA. Sulfuric acid (97%), ethanol (99.9%), and sodium hydroxide (NaOH) solution (1M) were obtained from Merck, Darmstadt, Germany. 4-(2-Hydroxyethyl)-1-piperazineethanesulfonic acid (HEPES) and sodium phosphate buffer (PBS, 10× concentrated) were purchased from Carl Roth, Karlsruhe, Germany. Hydrogen peroxide (30% w/v) was obtained from Fisher Scientific GmbH, Schwerte, Germany. Water was purified in TKA MicroPure Ultra Pure Water System produced by Thermo Fisher Scientific, Niederelbert, Germany. Borofloat wafers 4 in. (100 mm × 0.5 mm) were obtained from Plan Optik, Elsoff, Germany.

B. Microchannel fabrication

Microfluidic devices with three separate channels were fabricated using conventional microfabrication techniques. A schematic of the microchannel cross-section and a top-side optical micrograph are shown in Fig. 1. Briefly, 75 μm wide and 66 μm deep channels were fabricated using 4 in. ⟨100⟩ silicon wafers using lithographic patterning, deep reactive ion etching (DRIE), anodic bonding to a plain borofloat wafer and DRIE from the backside to create in- and outlet holes. Devices with channels of both 66 μm and 700 nm depth on the same chip were fabricated similarly by first patterning the shallow channels using photolithography and RIE followed by patterning the deep channels using photolithography and DRIE.

C. Surface modification of bonded silicon/glass microfluidic channels

Vapor phase deposition of APTMS was performed using microchannel devices that had been treated for 10 min with atmospheric plasma to clean the external surfaces.

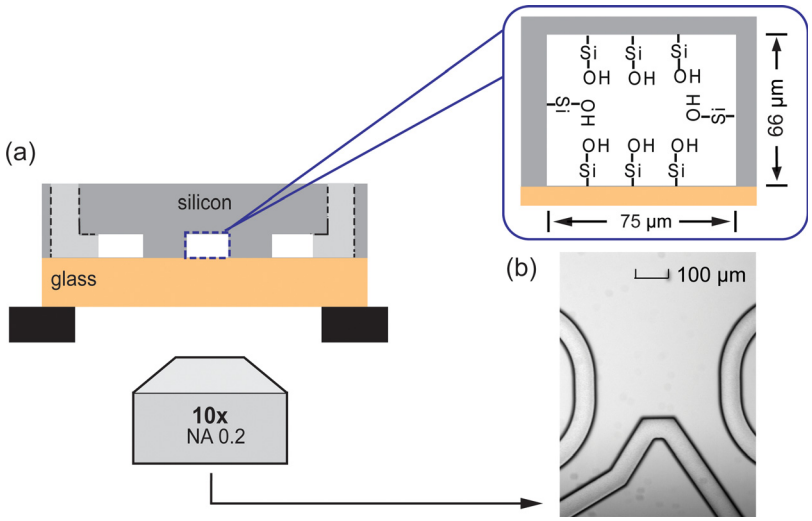

FIG. 1. Cross section schematic (a) and bright field image (b) of a microchannel device with channel width of 75 μm and channel height of 66 μm.

✓ To avoid trace amount of water, the transfer of 3 μl APTMS into 10 ml vials was conducted in an argon filled glove bag, Carl Roth, Karlsruhe, Germany.

The capped glass vials were then incubated at 80 °C under argon for 16 h. Afterwards, the devices were removed from the glass vials and connected to a pressure controlled fluidic manifold. All channels were then rinsed thoroughly with ethanol and dried with nitrogen gas. To maintain an unsilanized reference channel, the inlets of one channel were protected with Kapton® tape. All tape was removed prior to rinsing with ethanol.

Vapor phase silanization was also performed on borofloat glass slides (ca. 9 mm × 12 mm). The slides were initially cleaned in piranha solution (2:1 sulfuric acid/hydrogen peroxide) for a minimum of 30 min. The slides were then thoroughly rinsed with pure water, dried under nitrogen gas, and plasma treated for 10 min. To maintain an area of the slides unsilanized, one half on both sides of the slide was covered with Kapton® tape.

□ Caution: piranha solution is a strong oxidizer and is extremely corrosive.

D. Fluorescence labeling of surface functional groups

Fluorescence labeling of amine modified surfaces was performed using Alexa Fluor® 555 carboxylic acid succinimidyl ester (AF555-NHS-ester) alone (5 and 10 μM) or with a mixture of AF555-NHS-ester and EZ-Link® sulfosuccinimidyl 6-(biotinamido) hexanoate (sulfo-NHS-biotin) as illustrated in Fig. 2. Mixtures were prepared from the solutions of AF555-NHS-ester (70-350 μM) and sulfo-NHS-biotin (5-5.5 mM) in 10 mM HEPES buffer at pH 8.

✓ It is important to prepare all the solutions fresh to minimize the hydrolysis of the NHS esters.

☞ Total solution concentration of NHS esters was kept constant at 5 mM for all the mixtures while varying the stoichiometry of AF555-NHS-ester and sulfo-NHS-biotin.

The resulting AF555-NHS-ester concentration in each solution mixture ranged from 1.25 μM to 40 μM and the corresponding mole fraction was 0.025% to 0.8%. The silanized microfluidic channels were labeled by continuously flowing 150 μl of NHS ester solution through the channel for 60 min at room temperature in a dark room. After labeling, the channels were rinsed with HEPES buffer and water before drying with nitrogen gas.

✓ Based on the detection over a wide range of labeling concentrations, we set the standard mixture solution of 2.5 μM AF555-NHS-ester (the mole fraction of 0.025%) and 5 mM sulfo-NHS-biotin for direct quantification and real-time monitoring.

Functionalized glass slides were also labeled with the same concentrations of AF555-NHS-ester and sulfo-NHS-biotin. Slides were sandwiched between two glass coverslips with 30 μl of solution covering each side and incubated at room temperature for 60 min. The slides were then rinsed with water and dried with nitrogen gas.

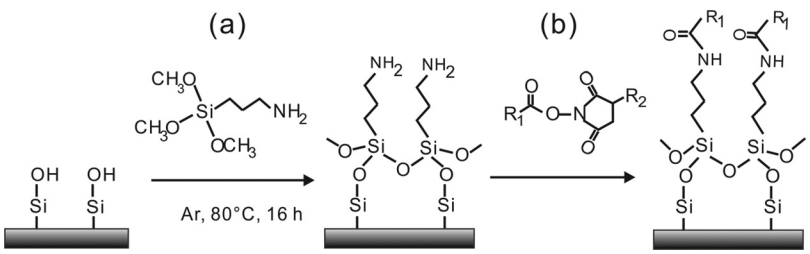

FIG. 2. Reaction schematic for covalent attachment of NHS-based molecules to silicon and glass substrates. (a) Vapor phase deposition of APTMS; (b) amine coupling of AF-NHS-ester (R_1 = Alexa Fluor® 555; R_2 = H) and/or sulfo-NHS-biotin (R_1 = LC-biotin; R_2 = -SO_3^-).

E. Fluorescence imaging and intensity measurement

All fluorescence experiments were conducted in microfluidic channels under buffer flow unless otherwise specified. The device was mounted onto an inverted microscope (Zeiss Axio Observer D1m, Germany) with a 10×, 0.2 NA objective and fluorescence images were captured with a CCD camera (Andor Clara, Andor Technology, N. Ireland). Alexa Fluor® 555 was excited at 537 ± 25 nm and the emission was observed at 610 ± 96 nm (Zeiss filter set 75 HE 489075). Controlled fluid flow was achieved by pressurizing the headspace of sealed autosampler vials. Fluorescence images were acquired with an exposure time of 1 s. Fluorescence intensity of each channel was analyzed with Image J (National Institute of Health, USA). Each experimental condition was performed in triplicate. Non-specific adsorption of AF555-NHS-ester was controlled by simultaneously monitoring the fluorescence in reference channels. The intensity from the reference channel was used as background and subtracted from fluorescence measurements of the other channels in the same image.

Fluorescence intensity measurements were calibrated using known AF555-NHS-ester concentrations in a microfluidic channel of defined depth. All molecules within the channel are assumed to contribute equally to the fluorescence signal due to the large depth of field of the 10× microscope objective used.

F. Fluorospectrometer measurements

A NanoDrop 3300 fluorospectrometer (Thermo Fisher Scientific GmbH, Germany) was used to measure the concentration of fluorescent molecules cleaved from borofloat glass slides. To remove bound fluorophores from the surface, the slides were incubated at room temperature in 60 μl of 0.1 M NaOH. In addition, the fluorophore concentrations were calibrated with known AF555-NHS-ester concentrations in 0.1 M NaOH solution. Fluorescence emission was measured using the white light-emitting diode (LED) excitation source (500-680 nm) of the NanoDrop with emission monitored at 565 nm.

G. Surface stability measurements

Microfluidic channels were silanized with APTMS as described earlier and labeled with the standard mixture of 2.5 μM AF555-NHS-ester and 5 mM sulfo-NHS-biotin. The samples were then exposed to various conditions including 0.1 M NaOH solution, water, and PBS buffer (pH 7.4). Each solution was tested in a separate channel. Channels were exposed for six 10 min intervals with each solution, and between each interval the solutions were changed to HEPES buffer for fluorescence imaging. All images were acquired at 1 s exposure time on the CCD. Each condition was tested for a total of 60 min. All experiments were done in triplicate, and the relative fluorescent intensities were normalized by the starting intensity.

H. X-ray photoelectron spectroscopy analysis

Surface characterization was performed on open silicon substrates using a PHI 5500 Multi-Technique X-ray photoelectron spectrometer system from Perkin-Elmer equipped with a Mg K X-ray source with energy of 1253.6 eV. The elemental composition of samples was obtained from survey spectra, collected at pass energy of 187.85 eV.

III. RESULTS

A. Elimination of self-quenching for fluorescence quantification of surface amine groups

Initially, to validate the success of silanization in the microchannel, we labeled the surface with a pure solution of AF555-NHS-ester (Fig. 3(a)). The fluorescence intensity measured for labeling concentrations of 5 and 10 μM showed no change, suggesting that surface saturation had been reached. Interestingly, under constant illumination it was observed that the

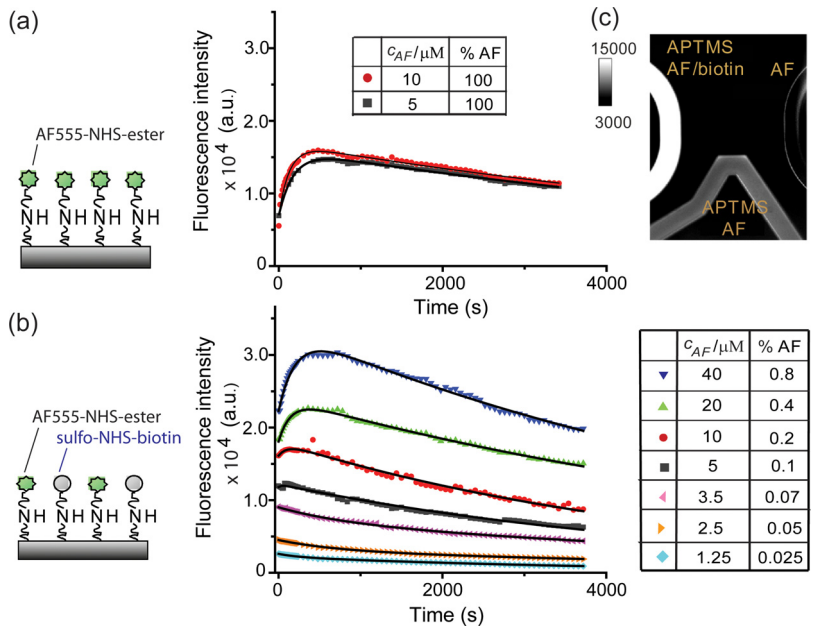

FIG. 3. Fluorescent intensity profiles and concentration tables for microchannels immobilized with (a) AF555-NHS-ester alone and (b) mixtures of AF555-NHS-ester and sulfo-NHS-LC-biotin. Solid lines represent the least squares fits according to Eq. (1). Non-monotonic fluorescence signal traces observed on the densely labeled surface within the first 500 s are due to the opposing effects of self-quenching and photobleaching. (c) Fluorescent image at time zero of three microchannels silanized and labeled with AF555-NHS-ester (5 μM) and sulfo-NHS-LC-biotin (5 mM) (left); silanized and labeled with AF555-NHS-ester (5 μM) alone (middle); unsilanized and labeled with AF555-NHS-ester (5 μM) alone (right).

fluorescence intensity rose for the first ~500 s before exhibiting a continual decrease. This behaviour may be attributed to the combination of self-quenching and photobleaching.

In general, self-quenching of closely packed fluorescent molecules poses an important challenge for the accurate quantification of surface coverage.[34] We have explored the potential to mitigate self-quenching by controlling the distance between immobilized fluorescent molecules. To achieve this, a non-fluorescent competitor, sulfo-NHS-biotin, was introduced into the AF555-NHS-ester solution to dilute the surface concentration of fluorescent molecules.

Although our work does not make use of the functionality of biotin, sulfo-NHS-biotin was selected for its similar size, good solubility, and expected similar reaction kinetics comparable with AF555-NHS-ester. In order to simplify the quantification of the bound molecules it is convenient to choose a competitor with the same coupling chemistry as the fluorescent label. In addition, if the rate of binding is reaction rather than diffusion limited, this ensures that the amount of bound species will only depend on their relative concentrations in solution and differences in molecular weight will have a minor effect. This condition of reaction limited binding is easily fulfilled for the coupling of NHS-ester to reactive amine groups, as experimentally determined under similar pH and temperature conditions.[35–37]

The effect of limiting the fluorescent labeling density was observed by comparing the brightness of the three channels in Fig. 3(c). The left channel was labeled using a solution of 5 μM AF555-NHS-ester in a background of 5 mM sulfo-NHS-biotin, while both the middle channel and the unsilanized right reference channel were exposed to 5 μM AF555-NHS-ester alone. Fluorescence in the unsilanized reference channel remained unchanged after incubation of AF555-NHS-ester alone, indicating that non-specific adsorption was below the detection limit. At the initial point of exposure, higher intensities were observed in the sparsely labeled left channel compared to the middle channel. This relationship then reverses after prolonged illumination (supplementary Fig. S-1),[46] indicating that under heavy labeling conditions quenching is present.

Time course measurements of fluorescent intensity for various AF555-NHS-ester and sulfo-NHS-biotin concentration ratios are shown in Fig. 3(b). The total concentration of both species

was maintained at 5 mM to minimize potential differences in labeling efficiency. The fluorescence intensity decreases monotonically with illumination time at low concentration ratios of AF555-NHS-ester (0.025% to 0.1%). However, for higher ratios (≥0.2%), a similar trajectory to Fig. 3(a) can be observed and this non-monotonic behaviour becomes more evident as the concentration of AF555-NHS-ester increases.

Fluorescence intensity as a function of time can be well fitted with Eq. (1)

$$I = \left(A_1 e^{-t/\tau_{ph1}} + A_2 e^{-t/\tau_{ph2}}\right)\left(1 - A_3 e^{-t/\tau_{dequench}}\right). \quad (1)$$

Here, the first factor refers to the photobleaching intensity decay with time constants τ_{ph1} and τ_{ph2}. Two time constants are included, since photobleaching is sensitive to the chemical environment of the dye and has been seen to follow multi-exponential behavior, particularly in the case of bound molecules.[38–41] The second factor represents the decrease in intensity due to the fraction (A_3) of quenched fluorophores that leave their quenched state with time constant τ_{dequench}. Fits to our experimental data using this equation showed that for fluorophore concentrations lower than 3.5 μM, $A_3 = 0$, whereas for higher dye concentrations $A_3 \neq 0$ (supplementary Table S-I),[46] within the error of the fit. The fitted results are depicted as continuous lines in Fig. 3(b), and the related parameters and corresponding fit errors and R^2 values are provided in the supplementary material (Tables S-I and S-II).[46] It is interesting to note that the fits show a dependence of the time constants, in particular τ_{ph2}, on the bound fluorophore density. This may be due to differences in the microenvironment at different surface coverage. The mechanisms behind self-quenching, in general, are complex and highly system-dependent[33] and the exact nature of the bound fluorophore's quenched state was not investigated further in this study. In the absence of self-quenching, the fluorescence signal increases in direct proportion to fluorophore surface coverage (Fig. 4(a)). The small deviations from linearity are likely due to variations in concentration during preparation caused by hydrolysis. In contrast, the fluorescence intensity of surfaces labeled with mixture solutions that have larger fluorophore fractions deviate significantly from linearity (supplementary Fig. S-2).[46]

Fluorescence intensity as a function of fluorophore concentration was calibrated using solutions of known AF555-NHS-ester concentrations inside the microchannels (Fig. 4(a) inset). Using this calibration, the measured density of AF555 molecules on the surface, $\sigma_{AF,measured}$, was obtained and the total area density of amine groups, $\sigma_{total,measured}$, was then calculated using

$$\sigma_{total,measured} = \frac{\sigma_{AF,measured} * (c_{AF} + c_{biotin})}{c_{AF}}, \quad (2)$$

where c_{AF} and c_{biotin} are the labeling concentrations of AF555-NHS-ester and sulfo-NHS-biotin, respectively. This equation assumes that since both species undergo the same chemical reaction and their binding rate is reaction limited, therefore the amount of each bound species is well approximated by the relative concentrations of ligands in solution. A correction for the case where the two ligands have different binding kinetics is given in the supplementary material.[46] Using Eq. (2), an average amine coverage of 55 ± 9 pmol/mm^2 was obtained. This result was independent of the exact ratio of AF-NHS-ester and sulfo-NHS-biotin for mixtures in the range $c_{AF} = 1.25$ μM to $c_{AF} = 3.5$ μM (Fig. 4(b)). Similar results were obtained when the experiment was conducted in nanofluidic channels with 700 nm height. Interestingly, it has been reported that the detected emission intensity can indeed be enhanced by more than two-fold in channels that approach 200 nm or below in both width and depth,[42] and researchers considering fluorescence quantitation in such channels should be mindful of this phenomenon.

The measured surface coverage is consistent with the reported amine density (3–50 pmol/mm^2) for an open silicon surface measured after cleavage of labeled molecules with UV/VIS detection.[43,44] In contrast, by labeling with fluorescent AF555-NHS-ester alone, initial intensities would

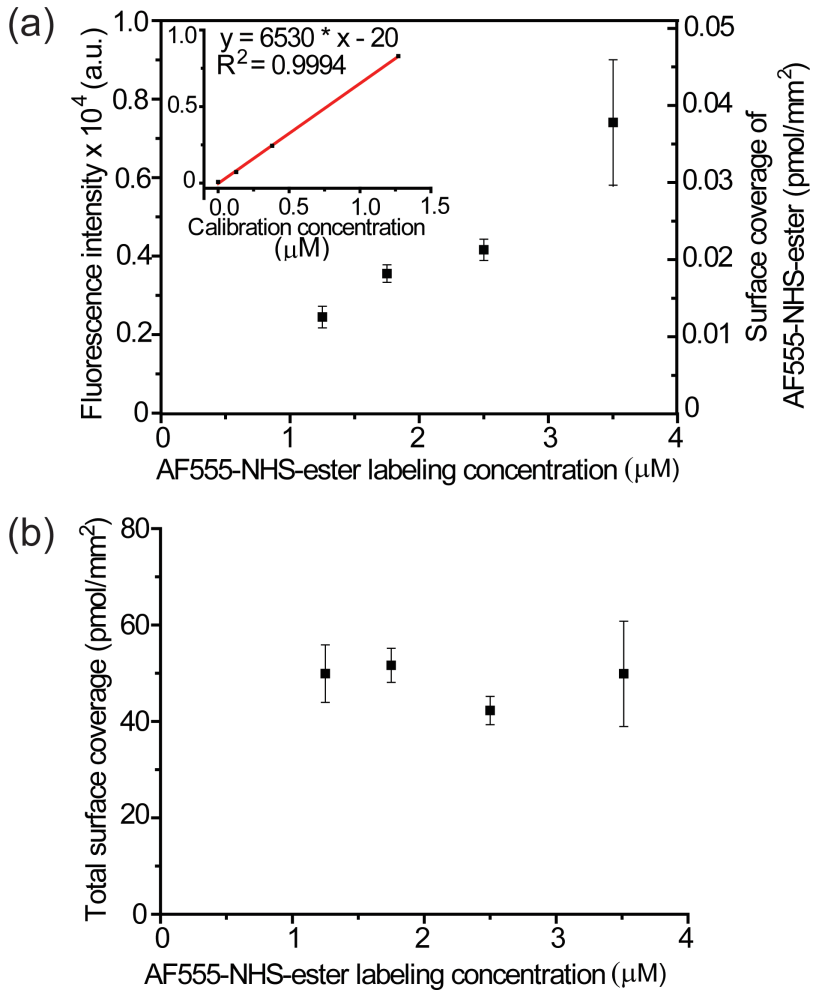

FIG. 4. (a) Fluorescence intensity and the corresponding surface coverage of different AF555-NHS-ester concentrations resulting from the competitive surface reaction. (Inset) Calibration plot of fluorescence intensity versus concentration. (b) Calculated total surface coverage of the microchannels using Eq. (2). Error bars indicate ±1 standard deviation calculated from triplicate experiments.

only correspond to 0.12 to 0.15 pmol/mm^2-values that are at least an order of magnitude less than the true surface coverage. To further corroborate the reliability of our quantification method, we also performed vapor phase APTMS silanization on open borofloat glass slides (~240 mm^2) and quantified the surface coverage again by cleaving the labeled molecules and detecting with a fluorospectrometer. The total calculated surface coverage of 63 ± 21 pmol/mm^2 is consistent with our microscopy-based measurements of labeled surfaces inside the microchannels. Here, the measured surface coverage represents the effective number of accessible reactive sites only, while some of the amine groups embedded in the aminosilane multilayer are inaccessible to surface labeling.

B. Surface stability monitoring

The stability of amine functionalized microchannel surfaces under different solution conditions was monitored using real-time fluorescence imaging. The microchannels were labeled with the standard mixture of 2.5 μM AF555-NHS-ester and 5 mM sulfo-NHS-LC-biotin and then continuously rinsed with the buffer solution. Fig. 5 shows the fluorescence intensity change of labeled amine modified surfaces for the conditions of 1× PBS (pH 7.4), pure water, and 0.1M NaOH (pH 13). The fluorescence intensity remains

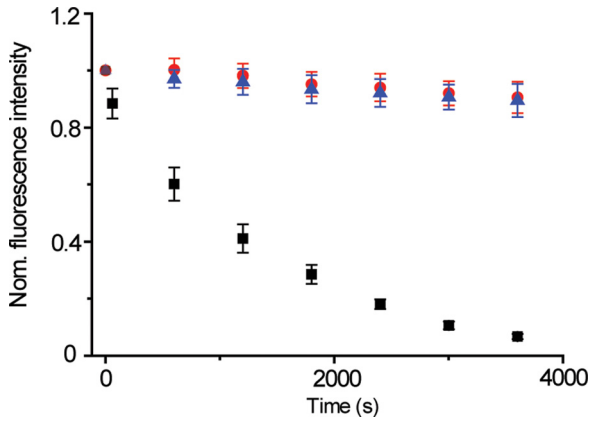

FIG. 5. Time-dependent stability measurements of APTMS modified surface rinsed with PBS buffer with pH 7.4 (●), pure water (▲), and 0.1 M NaOH (■). Measurements were taken by temporarily changing the solution in the channels to HEPES buffer at pH 8. Error bars indicate ±1 standard deviation calculated from triplicate experiments.

stable for both PBS and water but decreases quickly in the presence of 0.1M NaOH with a half-life of ∼16 min.

In addition, we characterized identically prepared open silicon surfaces with XPS. Table I shows the relative chemical composition of the APTMS modified substrates after incubation in different solutions and representative survey spectra are shown in Fig. S-3 in the supplementary material.[46] Initially, plasma treated surfaces resulted in 50.5 atomic percent (at. %) oxygen from the oxide layer. At the same time, 24.5 at. % silicon was present, along with 24.8 at. % carbon and negligible nitrogen. Surfaces functionalized with APTMS and incubated one hour in PBS resulted in a significant increase in nitrogen to 1.5 at. % with an uncertainty of ±0.2 at. % (error estimated from background on clean silicon surfaces). Surfaces treated with 0.1M NaOH solution for 60 min resulted in a substantial decrease in nitrogen content (0.1 at. %). As elemental nitrogen can be present only on the aminosilane deposited surfaces (Fig. 2), the nitrogen composition is here used as indicator for amine groups. The results verify the stability of the surface bound amine groups in PBS as well as their instability in the basic NaOH solution. Furthermore, these results also confirm that the decrease in fluorescence intensity for surfaces exposed to NaOH (Fig. 5) can be attributed to a degradation of the silane layer itself and not to the loss of fluorophore emission.

C. Quantification of vapor deposited monoalkoxyaminosilane

The utility of our method was further demonstrated by comparing aminosilane surface coverage of APTMS and APDMMS. Monoalkoxysilanes have the advantage of uniformity as they form a self-assembled monolayer on glass surfaces.[45] The surface coverage was quantified using the standard labeling condition identical to those used in the stability tests. Our result shows that APDMMS modified surface has 75% less accessible amine groups bound compared to the APTMS surface (Fig. 6).

TABLE I. XPS atomic concentrations of APTMS modified surfaces after incubation in different solutions. Atomic concentrations of nitrogen were used to indicate the presence of amine functional groups. The error in N (at. %) is estimated at 0.2 at. % based on the background of non-functionalized, plasma treated silicon surfaces.

Surface	O (at. %)	N (at. %)	C (at. %)	Si (at. %)
Si plasma treated	50.5	0.2	24.8	24.5
Si-APTMS, PBS incubation	41.5	1.5	34.1	22.9
Si-APTMS, NaOH incubation	17.5	0.1	22.4	60.0

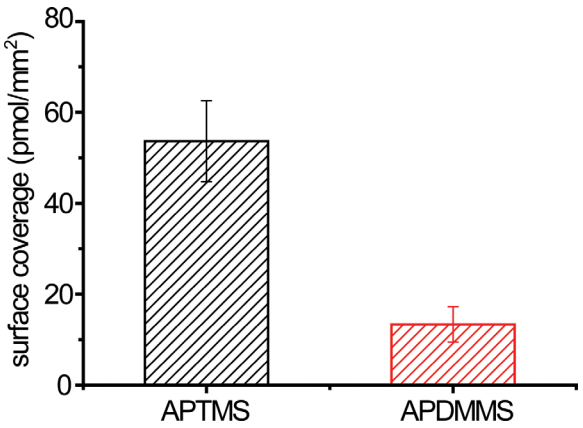

FIG. 6. Plot showing the total surface coverage for microchannel surfaces modified with aminoalkoxysilanes APTMS and APDMMS. Error bars indicate ±1 standard deviation calculated from triplicate experiments.

IV. CONCLUSIONS

Here, a simple and robust method was developed to allow quantitation of surface functional groups in closed micro and nanofluidic systems by fluorescence imaging. Fluorescence quenching at a high density of functional groups is avoided by a competitive labeling scheme which provides a linear relationship between fluorescence intensity and surface coverage. Within the linear range, the estimated silane coverage is insensitive to the exact concentration of fluorescent and non-fluorescent molecules and only requires precise control of the ratio. Furthermore, the method can be readily used to monitor surface stability in real-time. While one limitation of the method is the need for permanent chemical modification of the surface, choice of an appropriate competitor, such as NHS-biotin, in principle allows further derivatization without prior regeneration. Alternatively, a dedicated channel for characterization could be added to microfluidic devices to conduct representative measurements in batch modifications. The methods developed here are applicable to any silicon/glass based micro and nanofluidic system and could be expanded to silanes with different functionalities without the need of any specialized equipment.

ACKNOWLEDGMENTS

The authors would like to thank Professor Dr. Claus-Peter Klages and Sven Hartwig at the Fraunhofer Institute for Surface Engineering and Thin Films IST for carrying out the XPS measurements. We also thank Professor Dr. U. Benjamin Kaupp and Manfred Lacher for their generous support of the microfabrication work done at the Research Center Caesar. Funding for this work was provided by the Max Planck Society and the Max Planck Institute for Biophysical Chemistry. This work was partially supported by the German Federal Ministry of Education and Research (BMBF) under Grant No. 031A159.

[1]P. Yager, T. Edwards, E. Fu, K. Helton, K. Nelson, M. R. Tam, and B. H. Weigl, Nature **442**, 412 (2006).
[2]S. Haeberle and R. Zengerle, Lab Chip **7**, 1094 (2007).
[3]C. Y. Lee, P. Gong, G. M. Harbers, D. W. Grainger, D. G. Castner, and L. J. Gamble, Anal. Chem. **78**, 3316 (2006).
[4]T. P. Burg, M. Godin, S. M. Knudsen, W. Shen, G. Carlson, J. S. Foster, K. Babcock, and S. R. Manalis, Nature **446**, 1066 (2007).
[5]C. Jonsson, M. Aronsson, G. Rundstrom, C. Pettersson, I. Mendel-Hartvig, J. Bakker, E. Martinsson, B. Liedberg, B. MacCraith, O. Ohman, and J. Melin, Lab Chip **8**, 1191 (2008).
[6]A. H. C. Ng, U. Uddayasankar, and A. R. Wheeler, Anal. Bioanal. Chem. **397**, 991 (2010).
[7]K. C. Popat and T. A. Desai, Biosens. Bioelectron. **19**, 1037 (2004).
[8]M. Viefhues, S. Manchanda, T. C. Chao, D. Anselmetti, J. Regtmeier, and A. Ros, Anal. Bioanal. Chem. **401**, 2113 (2011).
[9]H. Lee, S. M. Dellatore, W. M. Miller, and P. B. Messersmith, Science **318**, 426 (2007).
[10]T. L. Yang, S. Y. Jung, H. B. Mao, and P. S. Cremer, Anal. Chem. **73**, 165 (2001).
[11]C. J. Huang, K. Bonroy, G. Reekmans, W. Laureyn, K. Verhaegen, I. De Vlaminck, L. Lagae, and G. Borghs, Biomed. Microdevices **11**, 893 (2009).

[12]F. Persson, J. Fritzsche, K. U. Mir, M. Modesti, F. Westerlund, and J. O. Tegenfeldt, Nano Lett. **12**, 2260 (2012).
[13]N. R. Glass, R. Tjeung, P. Chan, L. Y. Yeo, and J. R. Friend, Biomicrofluidics **5**, 036501 (2011).
[14]J. H. L. Beal, A. Bubendorfer, T. Kemmitt, I. Hoek, and W. M. Arnold, Biomicrofluidics **6**, 036503 (2012).
[15]S. Fiorilli, P. Rivolo, E. Descrovi, C. Ricciardi, L. Pasquardini, L. Lunelli, L. Vanzetti, C. Pederzolli, B. Onida, and E. Garrone, J. Colloid Interface Sci. **321**, 235 (2008).
[16]F. Zhang, K. Sautter, A. M. Larsen, D. A. Findley, R. C. Davis, H. Samha, and M. R. Linford, Langmuir **26**, 14648 (2010).
[17]M. J. Zhu, M. Z. Lerum, and W. Chen, Langmuir **28**, 416 (2012).
[18]B. Bhushan, T. Kasai, G. Kulik, L. Barbieri, and P. Hoffmann, Ultramicroscopy **105**, 176 (2005).
[19]E. Metwalli, D. Haines, O. Becker, S. Conzone, and C. G. Pantano, J. Colloid Interface Sci. **298**, 825 (2006).
[20]S. Flink, F. C. J. M. van Veggel, and D. N. Reinhoudt, J. Phys. Org. Chem. **14**, 407 (2001).
[21]M. E. Vlachopoulou, A. Tserepi, P. Pavli, P. Argitis, M. Sanopoulou, and K. Misiakos, J. Micromech. Microeng. **19**, 015007 (2009).
[22]X. X. Zeng, G. H. Xu, Y. A. Gao, and Y. An, J. Phys. Chem. B **115**, 450 (2011).
[23]E. Milkani, C. R. Lambert, and W. G. McGimpsey, Anal. Biochem. **408**, 212 (2011).
[24]K. Cottier, M. Wiki, G. Voirin, H. Gao, and R. E. Kunz, Sens. Actuators B **91**, 241 (2003).
[25]D. G. Kurth and T. Bein, Angew. Chem., Int. Ed. **31**, 336 (1992).
[26]J. H. Moon, J. W. Shin, S. Y. Kim, and J. W. Park, Langmuir **12**, 4621 (1996).
[27]S. Pal, M. J. Kim, and J. M. Song, Lab Chip **8**, 1332 (2008).
[28]F. Darain, P. Yager, K. L. Gan, and S. C. Tjin, Biosens. Bioelectron. **24**, 1744 (2009).
[29]E. A. McArthur, T. Ye, J. P. Cross, S. Petoud, and E. Borguet, J. Am. Chem. Soc. **126**, 2260 (2004).
[30]X. D. Song and B. I. Swanson, Anal. Chim. Acta **442**, 79 (2001).
[31]Y. J. Xing and E. Borguet, Langmuir **23**, 684 (2007).
[32]X. W. Zhuang, T. Ha, H. D. Kim, T. Centner, S. Labeit, and S. Chu, Proc. Natl. Acad. Sci. U.S.A. **97**, 14241 (2000).
[33]R. F. Chen and J. R. Knutson, Anal. Biochem. **172**, 61 (1988).
[34]M. Rae, A. Fedorov, and M. N. Berberan-Santos, J. Chem. Phys. **119**, 2223 (2003).
[35]E. J. M. Tournier, J. Wallach, and P. Blond, Anal. Chim. Acta **361**, 33 (1998).
[36]O. G. Berg and P. H. Vonhippel, Annu. Rev. Biophys. Biophys. Chem. **14**, 131 (1985).
[37]G. W. Cline and S. B. Hanna, J. Org. Chem. **53**, 3583 (1988).
[38]L. L. Song, E. J. Hennink, I. T. Young, and H. J. Tanke, Biophys. J. **68**, 2588 (1995).
[39]T. Bernas, M. Zarebski, R. R. Cook, and J. W. Dobrucki, J. Microsc. **215**, 281 (2004).
[40]G. Szabo, P. S. Pine, J. L. Weaver, M. Kasari, and A. Aszalos, Biophys. J. **61**, 661 (1992).
[41]L. Kunz and A. J. MacRobert, Photochem. Photobiol. **75**, 28 (2002).
[42]F. Westerlund, F. Persson, A. Kristensen, and J. O. Tegenfeldt, Lab Chip **10**, 2049 (2010).
[43]J. H. Moon, J. W. Shin, and J. W. Park, Mol. Cryst. Liq. Cryst. A **295**, 185 (1997).
[44]J. H. Moon, J. H. Kim, K. Kim, T. H. Kang, B. Kim, C. H. Kim, J. H. Hahn, and J. W. Park, Langmuir **13**, 4305 (1997).
[45]B. Dorvel, B. Reddy, I. Block, P. Mathias, S. E. Clare, B. Cunningham, D. E. Bergstrom, and R. Bashir, Adv. Funct. Mater. **20**, 87 (2010).
[46]See supplementary material at http://dx.doi.org/10.1063/1.4802270 for time-based fluorescence images (Fig. S-1), time-dependent fitting parameters and error (Tables S-I and S-II), fluorescence correlation at higher labeling concentrations (Fig. S-2), discussion on calculation of surface coverage quantification, and XPS analysis (Fig. S-3).